

Creating Cosmetic Technology Referring to the Dynamic Behavior of Living Systems

Kouichi Asakura*

Faculty of Science and Technology, Keio University, Kanagawa, Japan

The 1977 Nobel Prize in Chemistry was awarded for the concept of dissipative structures, which describes self-organization in far-from-equilibrium systems. This concept explains how open chemical systems, maintained in far-from-equilibrium conditions, become unstable to fluctuations, allowing them to grow into self-organized states via irreversible entropy-producing dissipative processes. Not only living systems but also artificial chemical systems spontaneously generate dynamic behavior without violating the second law of thermodynamics, provided they are open to the outer environment and maintained in a far-from-equilibrium condition. Representative examples include chemical oscillations and chemical waves in the Belousov–Zhabotinsky reaction system and Turing pattern formations in the chlorite–iodide–malonic acid reaction system. Chiral symmetry breaking transition is also a phenomenon categorized as a dissipative structure. The growth of fluctuations in far-from-equilibrium conditions occurs not only for the concentration of chemical species in chemical reaction systems but also for the morphology of the interface. Examples include viscous fingering and spinodal dewetting. When cosmetics are applied to the skin, volatile ingredients evaporate from the applied layer. Additionally, the cosmetic layer is occasionally exposed to water. These processes frequently place the cosmetics in a far-from-equilibrium condition. Therefore, unexpected patterns from the viewpoint of equilibrium and near-equilibrium thermodynamics are frequently generated in the applied cosmetic layer. Thus, the development of techniques to control the dynamic behavior generated under far-from-equilibrium conditions has become an important technological innovation in cosmetic science and technology.

Key words: dissipative structures, self-organization in far-from-equilibrium systems, growth of fluctuations, spontaneous generation of dynamic behavior, irreversible entropy-producing dissipative processes, viscous fingering, spinodal dewetting, chemical oscillations, chemical waves, Turing pattern formations

1. Introduction

Cosmetics application, evaporation of volatile ingredients from the applied cosmetic layer, and their exposure to water result in far-from-equilibrium conditions. The 1977 Nobel Prize in Chemistry was awarded for the concept of

*Corresponding author: Kouichi Asakura (E-mail: asakura@applc.keio.ac.jp)

Faculty of Science and Technology, Keio University, 3-14-1, Hiyoshi, Kohoku-ku, Yokohama-shi, Kanagawa 223-8522, Japan

DOI: 10.69336/acst.Inv-2024-03



© The Society of Cosmetic Chemists of Japan 2025

This article is licensed under a Creative Commons Attribution 4.0 International License.

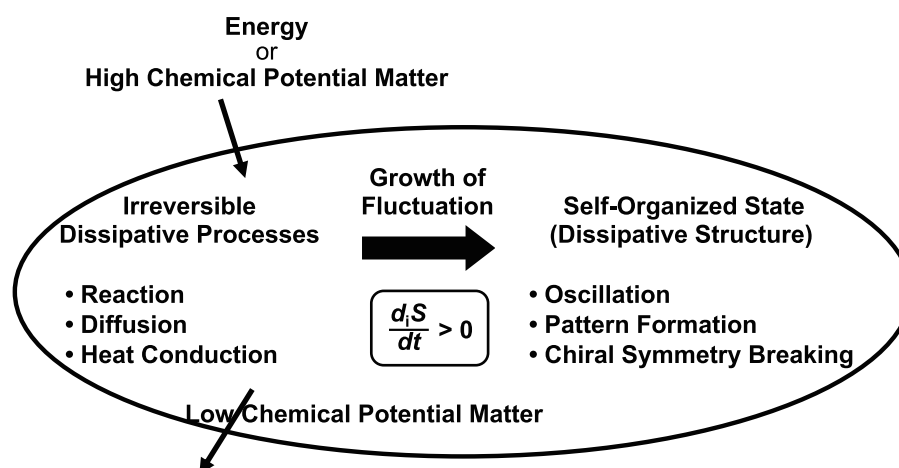


Fig. 1 Schematic illustration of the concept of dissipative structures, namely, self-organization in far-from-equilibrium systems.

dissipative structures, that is, self-organization in far-from-equilibrium systems.¹⁻³⁾ This concept explains how open chemical systems, maintained in far-from-equilibrium conditions, become unstable to fluctuations, allowing them to grow into self-organized states via irreversible entropy-producing dissipative processes. A characteristic feature of these self-organized states is the spontaneous generation of dynamic behaviors. No dynamic behavior is generated by self-assembly near equilibrium, such as in supramolecules. Living systems are representative examples of dissipative structures. They are open to the outer environment and are maintained under far-from-equilibrium conditions. In addition, metabolic processes always occur, and these processes are irreversible entropy-producing dissipative processes. Thus, living systems spontaneously exhibit dynamic behavior without violating the second law of thermodynamics. Both living and artificial chemical systems can spontaneously generate dynamic behaviors under far-from-equilibrium conditions. This review briefly explains the basic concept of dissipative structures. Additionally, we present the results of our recent research on cosmetic technologies based on this concept.

2. Dissipative Structure and Self-Organization in Far-from-Equilibrium Systems

Temporal patterns, such as cardiac pulsation and circadian rhythms, and spatial patterns, such as spatially periodic concentration patterns of animal skin pigments, are ubiquitous in living systems. The emergence of these dynamic patterns is neither a violation of the second law of thermodynamics nor a mystery of life. Ilya Prigogine, who was awarded the 1977 Nobel Prize in Chemistry, proposed the concept of dissipative structures to explain why these pattern formations are self-organized in far-from-equilibrium systems owing to the growth of fluctuations. As summarized in Fig. 1, when the system is open and maintained in far-from-equilibrium conditions by exchanging energy and matter with the outer environment, entropy-producing irreversible processes, such as reactions, diffusion, and heat conduction, allow fluctuations to grow and emerge as self-organized states, such as temporal oscillations, spatial pattern formation, and chiral symmetry breaking transitions.¹⁻³⁾ Living systems always take up high chemical potential matter, such as nutrients and oxygen, from the outer environment, transfer them to low chemical potential matter, such as carbon dioxide, and discard the low chemical potential matter to the outer environment. Living systems can generate dynamic behavior under these far-from-equilibrium conditions, and this is not a violation of the second law of thermodynamics.

Artificial chemical systems can also generate dynamic behavior under far-from-equilibrium conditions. Typical examples include chemical oscillations and chemical waves in the Belousov–Zhabotinsky (BZ) reaction system⁴⁾ (Figs. 2A, 2B). In this reaction system, high chemical potential organic compounds such as malonic acid ($\text{CH}_2(\text{COOH})_2$) and bromo malonic acid ($\text{BrCH}(\text{COOH})_2$), along with the oxidizing agent, bromate (BrO_3^-), are transformed into low chemical potential matter such as carbon dioxide (CO_2) (Fig. 2C). However, oxidation is not a simple chemical reaction like combustion. The BZ reaction system consists of a complex reaction network, similar to metabolic systems (Fig. 2C). Under conditions of abundant high chemical potential matter, the concentrations of intermediate species such as HBrO_2 and Br^- , and the ratio of oxidized to reduced metal ions, exhibit temporal oscillations and spatiotemporal pattern formation because of the growth of fluctuations in their concentrations.

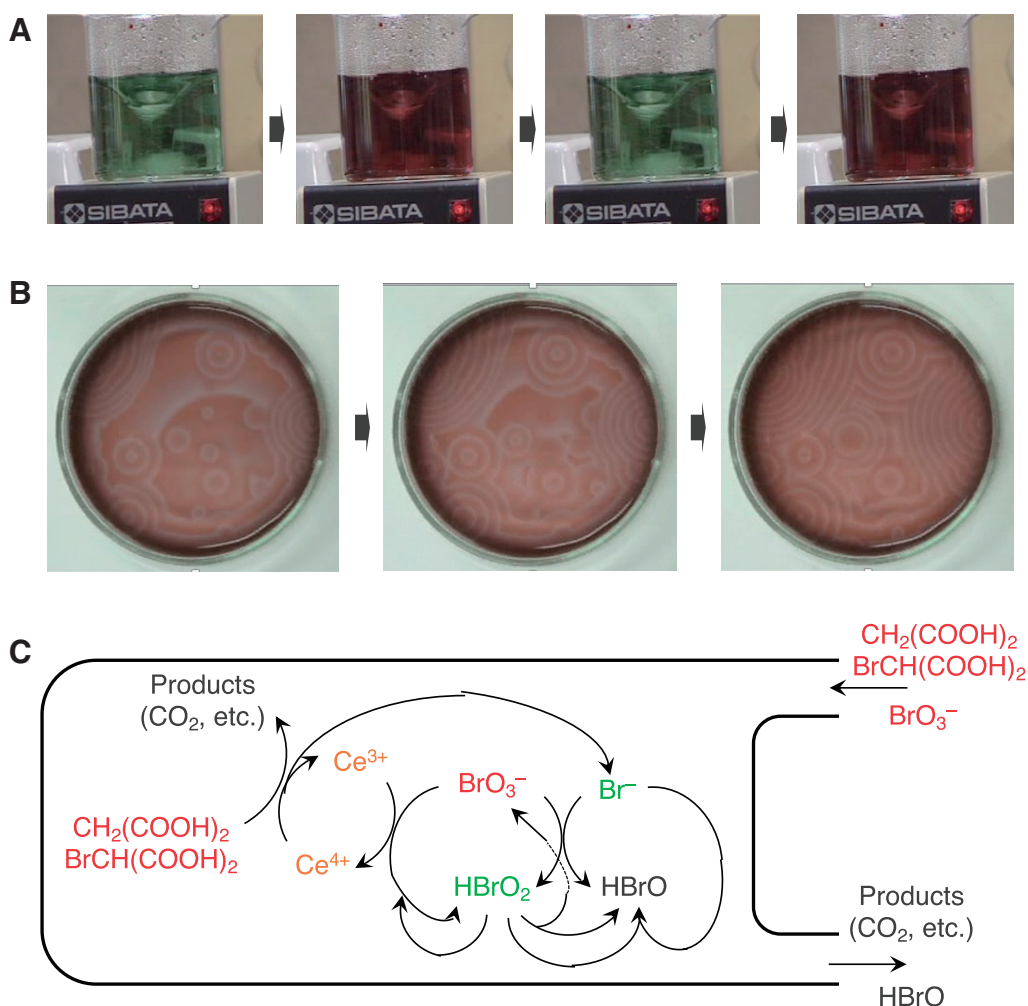


Fig. 2 BZ reaction system. (A) Chemical oscillation in the BZ reaction system. (B) Chemical waves in the BZ reaction system. (C) Mechanism of the BZ reaction system.

Another typical example of a dissipative structure is the Turing pattern. In 1952, Turing developed a theoretical model to explain how static, spatially periodic concentration patterns can spontaneously generate from the instability of a spatially homogeneous state by coupling nonlinear chemical reactions and diffusion.⁵⁾ The first experimental realization of the Turing pattern was achieved in 1990 in the chlorite–iodide–malonic acid reaction system.⁶⁾ The concentrations of intermediate chemical species in this system and their chemical potentials were spatially inhomogeneous in the Turing pattern (Fig. 3). Their generation and maintenance were supported by irreversible nonlinear chemical reactions and diffusion. These features are very different from those of self-assemblies near equilibrium, such as supramolecules.

We previously studied far-from-equilibrium phenomena in chemical reaction systems, such as chemical oscillation,^{7,8)} Turing pattern formation,⁹⁾ and chiral symmetry breaking transition.¹⁰⁾ Additionally, research on the dynamic behaviors of interfaces generated in far-from-equilibrium conditions and related issues has been conducted to develop innovative cosmetic technologies.^{11–29)}

3. Far-from-Equilibrium Pattern Formation by the Growth of Morphological Fluctuations in Interfaces

Many dynamic behaviors are spontaneously generated at the interface under far-from-equilibrium conditions, resulting in various patterns. Fingering instability occurs at the moving interface because of the growth of its morphological fluctuations. Representative examples include the formation of snow crystals, dendritic growth of bacterial colonies, and viscous fingering. In the case of viscous fingering,³⁰⁾ spatially periodic fingering patterns are typically generated because

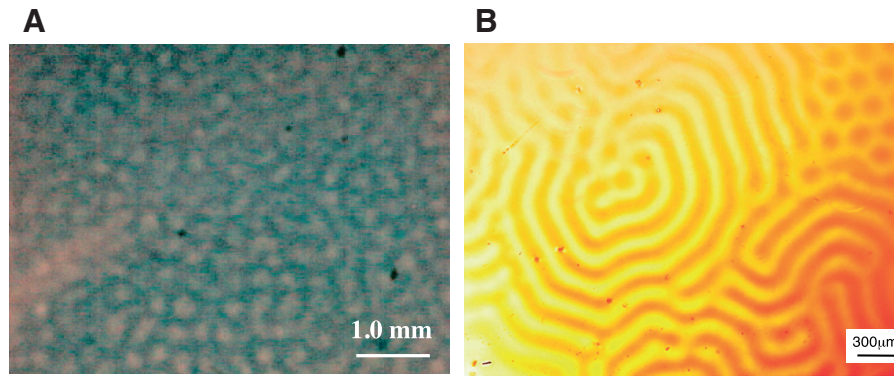


Fig. 3 Turing pattern formation in a CIMA reaction system. (A) shows the system in the aqueous solution of starch and (B) shows it in the polymer hydrogel consisting of the quaternary alkyl ammonium group. (Used with permission of American Chemical Society, from ref. 9. The final, published version of this article is available at <https://doi.org/10.1021/jp111584u>. Copyright©2011 American Chemical Society.)

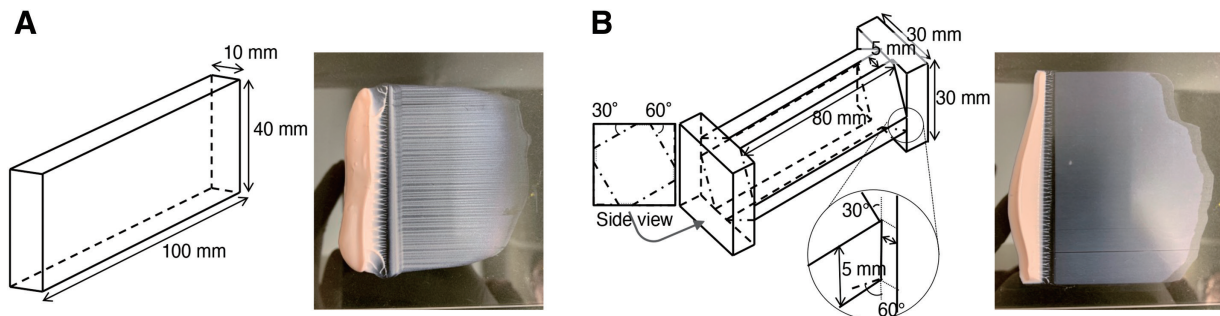


Fig. 4 Two types of applicators: (A) block applicator and (B) 4-sided applicator, for the application of sample liquid to generate (A) a spatially periodic stripe-patterned applied layer and (B) a flat-applied layer.¹⁶⁾ (Used with permission of Karger Publishers, from ref. 16. The final, published version of this article is available at <https://karger.com/?doi=10.1159/000356298>. Copyright©2014 Karger Publishers, Basel, Switzerland.)

the growth rate of a morphological fluctuation is a function of its wavelength, and the characteristic length of the spatial periodicity corresponds to the wavelength of the fastest-growing fluctuation.³¹⁾ For example, spatially periodic oil ripples are generated when a cylinder is rotated on the surface of the oil,³²⁾ and spatially periodic striped patterns are formed when 2 pieces of adhesive tape stuck together are peeled.^{33,34)} This phenomenon is called directional viscous fingering, and similar spatially periodic stripe patterns are typically formed when a viscous liquid is applied using a block applicator (Fig. 4A) or a cylindrical applicator.^{12–14)} However, a flat layer forms when a viscous liquid is applied using a 4-sided applicator^{16,17)} (Fig. 4B). In this case, the fingering pattern disappears as the liquid passes through the gap between the applicator and substrate.

Dewetting is another typical example of spatially periodic pattern formation under far-from-equilibrium conditions resulting from the growth of morphological fluctuations at the interface. It is a rupture of a thin liquid film on a solid substrate to generate holes when the spreading coefficient, $S = \Gamma_{SG} - (\Gamma_{SL} + \Gamma_{LG})$, where Γ_{SG} , Γ_{SL} , and Γ_{LG} are interfacial tensions between solid–gas, solid–liquid, and liquid–gas interfaces, respectively, changes its sign from positive to negative. Dewetting can be seen frequently when the volatile compound in the liquid film evaporates to change the value of Γ_{SL} and Γ_{LG} . It also occurs frequently when a hydrophobic liquid film formed on a hydrophilic substrate is exposed to water. In this case, the spreading coefficient becomes $S = \Gamma_{SW} - (\Gamma_{SL} + \Gamma_{LW})$, in which Γ_{SW} and Γ_{LW} are the interfacial tensions between solid–water and liquid–water interfaces, and Γ_{LW} is larger than Γ_{LG} to change the sign of the spreading coefficient, S , from positive to negative. The liquid film on the substrate is in a far-from-equilibrium condition when the spreading coefficient changes sign from positive to negative to undergo spinodal dewetting.³⁵⁾ Holes formed by spinodal dewetting show spatial periodicity because the growth rate of the morphological fluctuation is a function of its wavelength, similar to that of viscous fingering, and the characteristic length of the spatial periodicity corresponds to the wavelength of the fastest-growing fluctuation.³⁵⁾

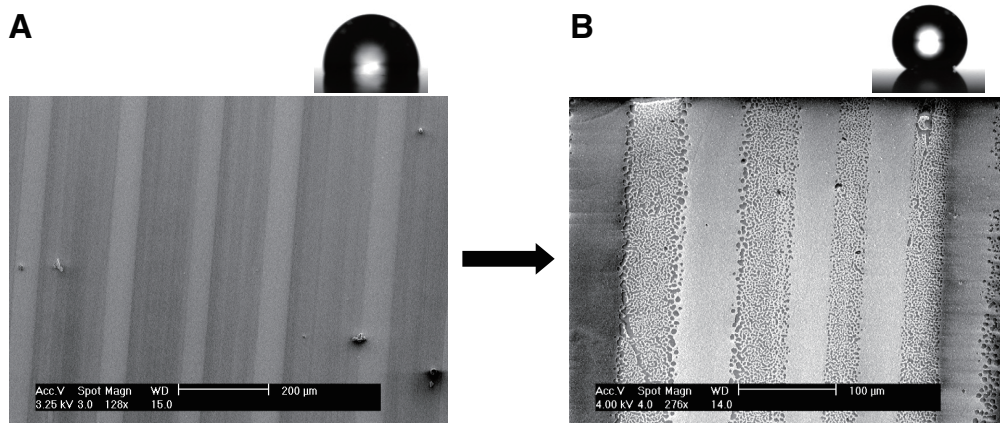


Fig. 5 (A) Stripe pattern formed on the applied layer of sample containing UV scattering agent and a UV absorber as a result of viscous fingering during its application. (B) Double-roughness structures, namely, coexisting mesoscopic spatially periodic stripe patterns and the microscopic dewetting patterns, formed on the sample layer by water shower treatment after its application to show highly water-repellent property.

4. Fabrication of Water-Repellent Surfaces by Utilizing Far-from-Equilibrium Interface Phenomena

Hydrophobic materials tend to enhance water-repellent properties when they possess surface roughness, according to Wenzel theory^{36,37} and Cassie theory.^{38,39} These theories, along with energy analysis, have predicted that double or multiple roughness are appropriate for making hydrophobic surfaces highly water-repellent. For instance, lotus leaves are known to possess mesoscopic protrusion structures ($\sim 20 \mu\text{m}$) and microscopic hairy structures ($0.2\text{--}1.0 \mu\text{m}$) that show a highly water-repellent property.⁴⁰ Attempts have been made to fabricate double-roughness surface structures using far-from-equilibrium pattern formation, directional viscous fingering, and spinodal dewetting to achieve this property.^{11–14} As this study was conducted to develop highly water-repellent sunscreens, octylsilyl titanium dioxide particles with an average diameter of 35 nm and 2-ethylhexyl methoxycinnamate were used as ultraviolet (UV) scattering agents and UV absorbers, respectively. They were mixed with decamethylcyclopentasiloxane, a volatile silicone. A linear motor coater was assembled from a linear motor actuator, and the sample was applied to a glass plate using a cylindrical applicator at a constant velocity.

Spatially periodic stripe patterns (Fig. 5A) were spontaneously formed on the applied sample layer because of directional viscous fingering when the application velocity was above a critical value. In contrast, a flat-applied layer was obtained when the application velocity was below a critical value, indicating that the application condition was far-from-equilibrium, which allowed morphological fluctuations in the interface to grow when the application velocity exceeded a critical value. However, no enhancement in the water-repellent properties was observed with the generation of this single submillimeter-scale surface roughness (Fig. 5A). Thus, we attempted to generate dewetting patterns on the sample layer by treating the sample with water. The water treatment was carried out by immersing the plate on which the sample was applied into a 35°C water shower for 1 min. A dewetting pattern was observed at the bottom part of the stripe pattern (Fig. 5B). Double-roughness structures, that is, coexisting mesoscopic spatially periodic stripe patterns and microscopic dewetting patterns, were formed by this simple method to demonstrate a highly water-repellent property (Fig. 5B). The technique developed in this study was applied to highly water-repellent sunscreens sold in 2003 and 2004.

5. Generation of Viscous Fingering during Sunscreen Application and Its Influence on the *In Vitro* Evaluation of UV-Protecting Ability

The UV-protecting abilities of sunscreens, as indicated by the sun protection factor (SPF)⁴¹ and UVA protection factor (UVA-PF),⁴² are evaluated using *in vivo* methods. These methods require UV irradiation of the human back. Thus, the need for establishing an *in vitro* evaluation method for UV protection has increased, as it provides results rapidly, ethically, and at a fraction of the cost. Although the ISO method for *in vitro* UVA-PF evaluation was approved in 2012,⁴³ it has not become the worldwide standard. Some countries do not admit indicating *in vitro* UVA-PF values for selling

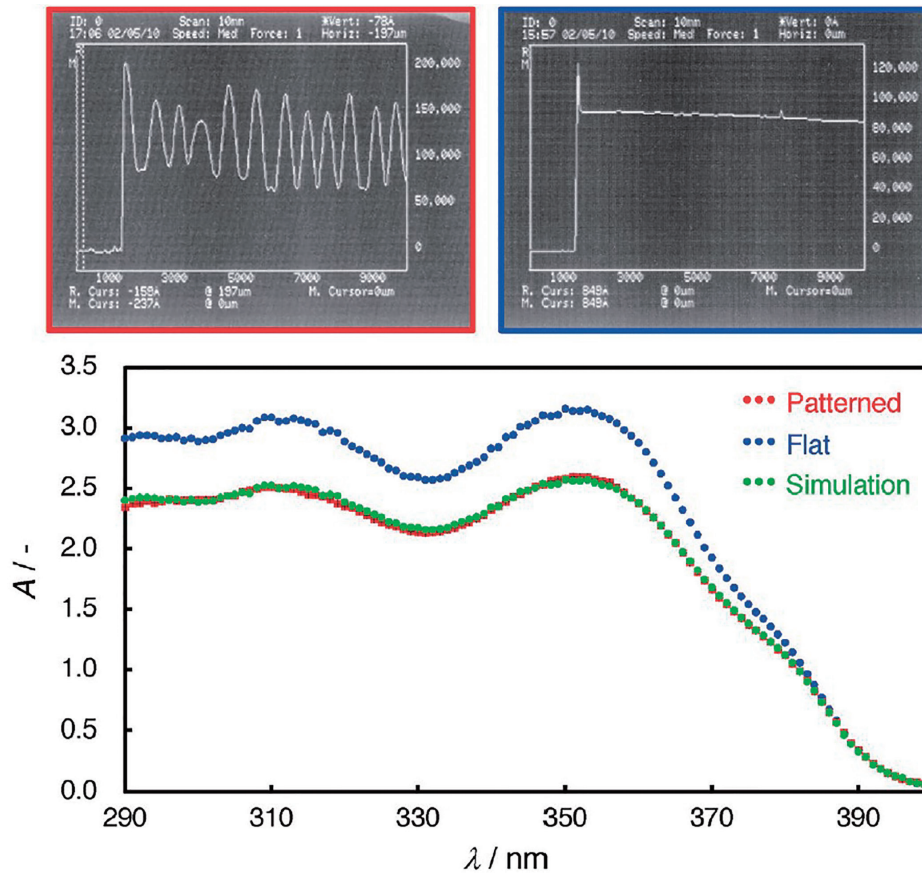


Fig. 6 UV absorption spectrum of the patterned and flat pseudo-sunscreen layer, which have almost identical average thickness at 11.8 and 11.5 μm , obtained using block applicator and a 4-sided applicator, respectively. Additionally, the UV absorption spectrum of the patterned pseudo-sunscreen layer was theoretically predicted from the thickness distribution data obtained by surface profile measurement, and the result was compared with the experimental results.¹⁸⁾ (Used with permission of the American Society of Photobiology, from ref. 18. The final, published version of this article is available at <https://onlinelibrary.wiley.com/doi/10.1111/php.12598>. Copyright©2016 The American Society of Photobiology, Herndon, USA.).

sunscreens because of its repeatability and reliability problems. Therefore, we analyzed the problems associated with the *in vitro* evaluation of UV-protecting ability of sunscreens.¹⁶⁻¹⁹⁾

When a striped pattern is formed in the sunscreen layer due to directional viscous fingering during application, the layer's thickness becomes spatially inhomogeneous. Theoretical analyses have shown that UV absorbance decreases as the distance between the top and bottom of a patterned sunscreen layer increases.^{16,17)} Experimental studies were performed to validate this theoretical prediction. A clear solution-type pseudo-sunscreen sample was prepared, in which diethylamino hydroxybenzoyl hexyl benzoate, butyl methoxydibenzoylmethane, and 2-ethylhexyl methoxycinnamate were dissolved. This sample was used to evaluate the influence of the geometric factor of the applied sample layer on the UV-protecting ability. The patterned and flat layers of the pseudo-sunscreen were formed using block and 4-sided applicators, respectively. The average thickness of each pseudo-sunscreen layer was almost identical (11.8 and 11.5 μm), and their UV-protecting abilities were compared. The UV absorbance of the patterned layer was significantly lower than that of the flat layer, and the UV absorption spectrum of the patterned layer, predicted from the thickness distribution data obtained from the surface profile measurements, matched the experimental results (Fig. 6).^{16,17)}

In 2011, the United States Food and Drug Administration launched a new rule using the term “Broad Spectrum” for labeling sunscreens.⁴⁴⁾ The critical wavelength is calculated from the UV absorption spectrum of the applied sunscreen layer, and the sample is approved as “Broad Spectrum Protection” if the critical wavelength is equal to or larger than 370 nm. Our theoretical analysis showed that the critical wavelength for the “Broad Spectrum” approval increases as the spatial inhomogeneity of the applied sunscreen layer increases.¹⁸⁾ From the UV absorbance data

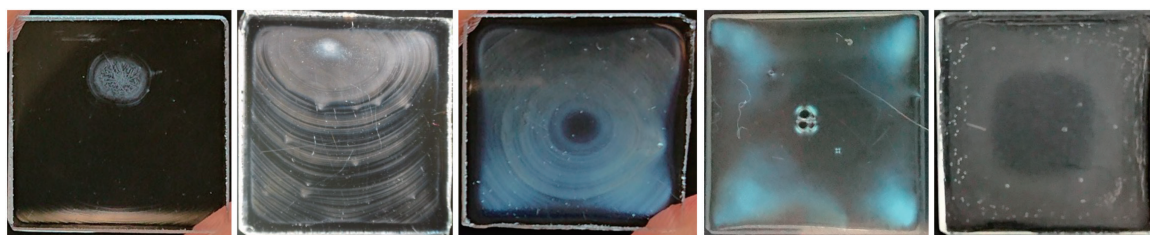


Fig. 7 Various kinds of non-flat and non-uniform hydroxyalkyl cellulose films usually formed during the evaporation of water from its aqueous solution spread on a square glass plate (2 cm × 2 cm)²². (Used with permission of the Japan Oil Chemists' Society, from ref 22. The final, published version of this article is available at <https://doi.org/10.5650/jos.ess21266>. Copyright©2022 Japan Oil Chemists' Society, Tokyo, Japan.).

shown in Fig. 6, the critical wavelength of the patterned layer was calculated to be 370 nm, whereas that of the flat layer was 369 nm. Therefore, the sunscreen sample that should not be approved as “Broad Spectrum Protection” was approved to have “Broad Spectrum Protection” due to the spontaneous stripe pattern formation during its application. Furthermore, “Broad Spectrum” testing⁴⁴) is carried out by applying a sunscreen sample on a standard roughened PMMA plate, according to the ISO *in vitro* UVA-PF evaluation method.⁴³) The spatial inhomogeneity of the sunscreen layer generated by viscous fingering and that generated for any reason increases the critical wavelength. We have found that the surface roughness of the standard roughened PMMA plate also causes the critical waves to increase, allowing the sunscreen sample that should not be approved as “Broad Spectrum Protection” to be approved as “Broad Spectrum Protection”.¹⁹)

6. Development of New *In Vitro* Evaluation Method of UV-Protecting Ability of Sunscreens and Its Validity

Recently, hydrophilic sunscreens, such as O/W emulsions, have become popular because of their smooth and light texture. However, they cannot wet the hydrophobic PMMA plate because they have high Γ_{LG} and Γ_{SG} , which make the spreading coefficient, S , negative. Therefore, attempts have been made to develop hydrophilic substrates that can be wetted with hydrophilic sunscreens. We succeeded in developing a superhydrophilic substrate with a water contact angle of 0° using a corona-discharge treatment on a flat quartz plate.^{20,21}) However, superhydrophilicity of the surface fabricated by this method was gradually lost during storage at 25°C, and the half-life of the contact angle of water was around 5 days. Thus, a superhydrophilic substrate should be freshly prepared immediately before use. This motivated us to develop another type of substrate with semi-permanent hydrophilicity. Attempts have been made to form hydroxyalkyl cellulose films on quartz plates.^{22,23}) Its aqueous solution was spread on a superhydrophilic quartz plate prepared by the corona-discharge treatment, and water was evaporated to form a hydroxyalkyl cellulose film. However, various drying patterns are usually formed in the hydroxyalkyl cellulose films during water evaporation (Fig. 7). The evaporation of volatile compounds from a thin liquid layer spreading on a solid substrate frequently causes far-from-equilibrium conditions to generate flow patterns, such as coffee rings^{45–48}) and Marangoni contractions.^{49–51}) Special care must be taken to avoid the generation of Marangoni flow, which leads to nonuniformity of the surface of the hydroxyalkyl cellulose film. We succeeded in developing a technique to fabricate flat hydroxyalkyl cellulose films with surface roughness below the μm level on a superhydrophilic quartz plate.^{22,23}) The contact angle of water on this substrate was determined to be $44 \pm 2^\circ$, and it scarcely varied during 6 months of storage.^{22,23})

A new *in vitro* UV-protecting ability evaluation method using a superhydrophilic plate (**SHP**), hydroxyalkyl cellulose film-coated plate (**HCC**), and **PMMA** plate (**PMMA**) was proposed (Fig. 8), and 6 sample sunscreens were evaluated.²²) Two of the 6 samples failed to wet **PMMA**, resulting in significantly lower UV absorbance compared to those applied to **SHP** and **HCC** (Fig. 9). Thus, **SHP** and **HCC** were found to be appropriate for the *in vitro* evaluation of UV-protecting ability of hydrophilic sunscreens. To standardize this test method, it is important that anyone can follow the instructions to perform the experiments at any place and obtain similar results. Additionally, the time and labor required for the experimenters are expected to be reduced. Therefore, we also proposed a simplified new *in vitro* UV-protecting ability evaluation method, and ring tests were performed by 3 experimenters at different laboratories in different organizations to inspect the usefulness of the method.²²) The coefficient of variation (the value dividing standard deviation by average) of *in vitro* SPF was less than 0.35 for 5 out of the 6 sunscreen samples (Table 1).

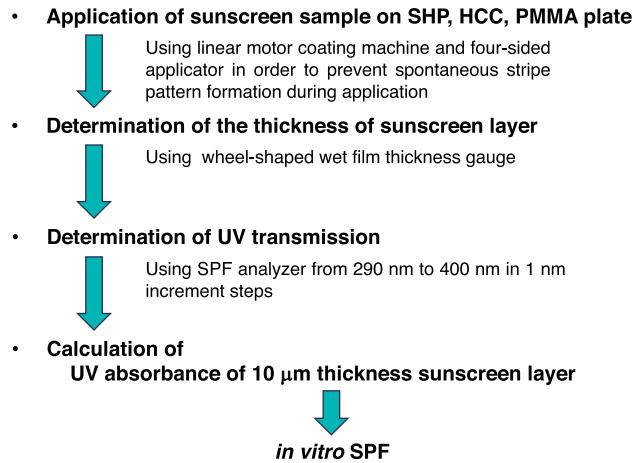


Fig. 8 Summary of the new *in vitro* UV protecting ability evaluation method for sunscreen samples²². (Used with permission of the Japan Oil Chemists' Society, from ref 22. The final, published version of this article is available at <https://doi.org/10.5650/jos.ess21266>. Copyright©2022 Japan Oil Chemists' Society, Tokyo, Japan.).

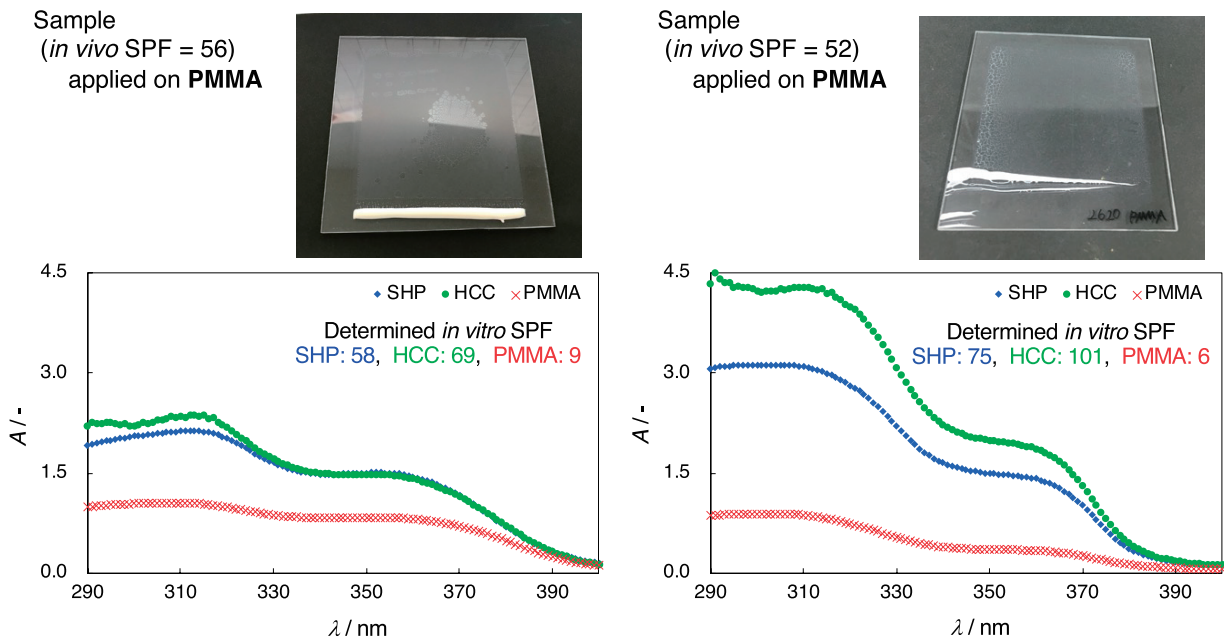


Fig. 9 Dewetting structure observed in the sunscreen layer applied on **PMMA** showing significantly low UV absorbance than that applied on **SHP** and **HCC**²². (Used with permission of the Japan Oil Chemists' Society, from ref 22. The final, published version of this article is available at <https://doi.org/10.5650/jos.ess21266>. Copyright©2022 Japan Oil Chemists' Society Tokyo, Japan.).

Table 1 Average (AVG), standard deviation (STD), and coefficient of variation (CV) of *in vitro* SPF of six sunscreen samples evaluated by the ring test²². (Used with permission of the Japan Oil Chemists' Society, from ref 22. The final, published version of this article is available at <https://doi.org/10.5650/jos.ess21266>. Copyright©2022 Japan Oil Chemists' Society, Tokyo, Japan.)

Sample	<i>in vivo</i> SPF	<i>in vitro</i>	
		AVG \pm STD	CV
1	56	101 \pm 30	0.30
2	55	103 \pm 31	0.30
3	52	100 \pm 15	0.15
4	25	15 \pm 8	0.57
5	15	12 \pm 3	0.23
6	4	7 \pm 2	0.34

7. Conclusion

Biomimetics is a field of research and development involving industrial technology. This study aimed to express a function similar to that of living systems by mimicking the molecular and assembling structures of materials and micro-morphological structures in living systems. However, few studies have been conducted on the expression of this function by mimicking the dynamic behavior spontaneously generated in living systems under far-from-equilibrium conditions. In this review, the concept of dissipative structures, that is, self-organization in far-from-equilibrium systems, is briefly explained, and our recent studies on dissipative structures in chemical reaction systems are introduced. In addition, we describe our efforts to develop a cosmetic technology based on the dynamic behavior of living systems. Self-assemblies near equilibrium, such as supramolecules, cannot spontaneously generate dynamic behavior, and biomimetics related to self-assembly near equilibrium cannot be used to study the dynamic phenomena that occur in cosmetics during use. Cosmetics are frequently used under far-from-equilibrium conditions. We believe that cosmetic technology, which refers to the dynamic behavior of living systems, can lead to important technological innovations.

Conflict of interest: There is no conflict of interest to declare.

Abbreviations: BZ, Belousov–Zhabotinsky; CIMA, chlorite–iodide–malonic acid; PMMA, poly(methyl methacrylate); SPF, sun protection factor; UV, ultraviolet; UVA-PF, ultraviolet A protection factor

References

- 1) G. Nicolis, I. Prigogine, Self-organisation in Non-equilibrium Systems: Towards a Dynamics of Complexity, in Bifurcation Analysis-Principles, Applications and Synthesis, ed. by M. Hazewinkel, R. Jurkovich, J. H. P. Paelinck, D. Reidel Publishing, Dordrecht, 1977, p.3–12
- 2) D.K. Kondepudi, I. Prigogine, Modern Thermodynamics: From Heat Engines to Dissipative Structure, John Wiley & Sons, Chichester, 1998
- 3) I.R. Epstein, J.A. Pojman, An Introduction to Nonlinear Chemical Dynamics: Oscillations, Waves, Patterns, and Chaos, Oxford University Press, New York, 1998
- 4) B.P. Belousov, “A periodic reaction and its mechanism” in Sbornik Referatov po Radiatsionni Meditsine, Med Publ., Moscow, 1958, p. 145
- 5) A.M. Turing, Philos. Trans. R. Soc. Lond., B, 237, 37–72 (1952)
- 6) V. Castets, E. Dulos, J. Boissonade, P. De Kepper, Phys. Rev. Lett., 64, 2953–2956 (1990)
- 7) S. Takayama, K. Okano, K. Asakura, Chem. Phys. Lett., 555, 300–305 (2013)
- 8) Y. Furue, K. Okano, T. Banno, K. Asakura, Chem. Phys. Lett., 645, 210–214 (2016)
- 9) K. Asakura, R. Konishi, T. Nakatani, T. Nakano, M. Kamata, J. Phys. Chem. B, 115, 3959–3963 (2011)
- 10) D.K. Kondepudi, K. Asakura, Acc. Chem. Res., 34, 946–954 (2001)
- 11) A. Kuroda, H. Takeshige, K. Asakura, J. Oleo Sci., 55, 277–282 (2006)
- 12) A. Kuroda, T. Ishihara, H. Takeshige, K. Asakura, J. Phys. Chem. B, 112, 1163–1169 (2008)
- 13) K. Asakura, A. Kuroda, H. Takeshige, T. Ishihara, Jpn. Pat., 5283819 (2013)
- 14) P. Joly, A. Kuroda, K. Asakura, J. Oleo Sci., 59, 89–94 (2010)
- 15) M. Endo, T. Mukawa, N. Sato, D. Maezawa, Y. Ohtsu, A. Kuroda, M. Wakabayashi, K. Asakura, Int. J. Cosmet. Sci., 36, 546–552 (2014)
- 16) K. Fujikake, S. Tago, R. Plasson, R. Nakazawa, K. Okano, D. Maezawa, T. Mukawa, A. Kuroda, K. Asakura, Skin Pharmacol. Physiol., 27, 254–262 (2014)
- 17) K. Asakura, A. Kuroda, Jpn. Pat. 5825654 (2015)
- 18) M. Wakabayashi, K. Okano, T. Mukawa, D. Maezawa, H. Masaki, A. Kuroda, K. Asakura, Photochem. Photobiol., 92, 637–643 (2016)
- 19) A. Kuroda, K. Sakai, S. Yahagi, T. Mukawa, N. Sato, N. Nakamura, D. Maezawa, H. Masaki, T. Banno, K. Asakura, J. Oleo Sci., 68, 175–182 (2019)
- 20) K. Asakura, A. Kuroda, IFSCC Magazine, 21, 53–57 (2018)
- 21) K. Asakura, A. Kuroda, WO2018/047707 (2018)
- 22) K. Ikawa, A. Aizawa, T. Banno, M. Fujishiro, S. Yahagi, A. Kuroda, K. Asakura, J. Oleo Sci., 71, 321–331 (2022)

- 23) A. Kuroda, WO2021/020432 A1 (2021)
- 24) S. Takekawa, M. Ohara, T. Banno, K. Asakura, *J. Oleo Sci.*, 70, 1081–1091 (2022)
- 25) S. Takekawa, M. Ohara, T. Banno, K. Asakura, *Int. J. Cosmet. Sci.*, 45, 38–49 (2023)
- 26) A. Aizawa, T. Banno, K. Asakura, *Langmuir*, 39, 16731–16739 (2023)
- 27) A. Aizawa, R. Sumita, T. Banno, K. Asakura, *J. Oleo Sci.*, 73, 593–601 (2024)
- 28) M. Fujishiro, S. Yahagi, A. Kuroda, T. Banno, K. Asakura, *J. Oleo Sci.*, 73, 603–610 (2024)
- 29) K. Asakura, A. Kuroda, M. Fujishiro, S. Yahagi, *J. Oleo Sci.*, 73, 121–134 (2024)
- 30) P. Saffman, G. Taylor, *Proc. R. Soc. Lond. A Math. Phys. Sci.*, 245, 312–329 (1958)
- 31) J.R.A. Pearson, *J. Fluid Mech.*, 7, 481–500 (1960)
- 32) V. Hakim, M. Rabaud, H. Thome, Y. Couder, Directional Growth in Viscous Fingering, in *New Trends in Nonlinear Dynamics and Pattern-Forming Phenomena*, ed. by P. Coulet, P. Huerre, Plenum Press, 1990, , p. 327–337
- 33) Y. Yamazaki, A. Toda, *J. Phys. Soc. Jpn.*, 71, 1618–1621 (2002)
- 34) Y. Yamazaki, A. Toda, *J. Phys. Soc. Jpn.*, 73, 2342–2346 (2004)
- 35) A. Vrij, *Discuss. Faraday Soc.*, 42, 23–33 (1966)
- 36) R.N. Wenzel, *Ind. Eng. Chem.*, 28, 988–994 (1935)
- 37) R.J. Wenzel, *J. Phys. Colloid Chem.*, 53, 1466–1467 (1949)
- 38) A.B.D. Cassie, S. Baxter, *Trans. Faraday Soc.*, 40, 546–551 (1944)
- 39) A.B.D. Cassie, *Discuss. Faraday Soc.*, 3, 11–16 (1948)
- 40) N.A. Patankar, *Langmuir*, 20, 8209–8213 (2004)
- 41) International Standards Organization, Cosmetics-Sun protection test methods-*In vivo* determination of the sun protection factor (SPF), ISO, 24444 (2010)
- 42) International Standards Organization, Cosmetics-Sun protection test methods-*In vivo* determination of sunscreen UVA protection, ISO, 24442 (2011)
- 43) International Standards Organization, Cosmetics-Sun protection test methods-Determination of sunscreen UVA photoprotection *in vitro*, ISO, 24443 (2012)
- 44) Department of Health and Human Services Food and Drug Administration, Sunscreen drug products for over-the-counter human use, *Fed. Regist.*, 76/117, 35620–35665 (2011)
- 45) K. Uno, K. Hayashi, T. Hayashi, K. Ito, H. Kitano, *Colloid Polym. Sci.*, 276, 810–815 (1998)
- 46) R.D. Deegan, O. Bakajin, T. F. Dupont, G. Huber, S. R. Nagel, T. A. Witten, *Nature*, 389, 827–829 (1997)
- 47) P.J. Yunker, T. Still, M.A. Lohr, A.G. Yodh, *Nature*, 476, 308–311 (2011)
- 48) H. Hu, R.G. Larson, *J. Phys. Chem. B*, 110, 7090–7094 (2006)
- 49) S. Karpitschka, F. Liebig, H. Riegler, *Langmuir*, 33, 4682–4687 (2017)
- 50) N.J. Cira, A. Benusiglio, M. Prakash, *Nature*, 519, 446–450 (2015)
- 51) H. Sadafi, S. Dehaeck, A. Rednikov, P. Colinet, *Langmuir*, 35, 7060–7065 (2019)